Egyptian Journal of Archaeological and Restoration Studies
An international peer-reviewed journal published bi-annually
www.ejars.sohag-univ.edu.eg

Original article

COMPARISON BETWEEN FOURIER TRANSFORM INFRARED SPECTROSCOPY AND ATTENUATED TOTAL REFLECTANCE-FOURIER TRANSFORM INFRARED SPECTROSCOPY (ATR-FTIR MAPPING) ON WOOD COVERED WITH GESSO LAYERS

Bayoumi, N.(*) & El Hadidi, N.

Organic Conservation dept., Faculty of Archaeology, Cairo Univ., Giza, Egypt
(*)E-mail address: Nohyr@cu.edu.eg

Article info.
Article history:
Received: 2-1-2025
Accepted: 15-3-2025
Doi: 10.21608/ejars.2026.499292

Keywords:
Lebanese cedar
Sidder
FTIR
ATR-FTIR mapping
Cellulose
Hemicellulose
Lignin

EJARS – Vol. SI (1) – April 2026: SI 51-SI 62

Abstract:
Throughout history wood was used as a support for polychrome layers. In ancient Egypt several types of gesso layers have been identified, and recent research has focused on how these layers may affect cellulose, hemicellulose and lignin, which are the main wood components. The chemical reactions between the main wood components of Lebanese cedar (Cedrus libani), sidder (Ziziphus spina-christi) wood and the different components of four commonly used preparation layers similar to those identified in the wooden artifacts in Tutankhamun's collection were studied on simulated samples by using both Fourier Transform Infrared spectroscopy (FTIR) and Attenuated Total Reflectance-Fourier Transform Infrared spectroscopy (ATR-FTIR Mapping) for the first time to study the chemical changes in the main function groups of wood. FTIR analysis demonstrated in detail the changes that occurred in wood chemical components. ATR-FTIR analysis helped explain what happens in wood surface, while FTIR mapping images showed the effect of preparation layers on the chemical components of wood, the results of which were correlated with the results of FTIR bands ratios. The results obtained clearly show that these analytical techniques can be easily applied on archaeological samples to assess the state of preservation of wooden supports.

1. Introduction

Howard Carter's astonishing discovery began with a candle held through a small hole in the blocked doorway of Tutankhamun's tomb on November 26, 1922 [1]. This tomb contained everything such as: the gold mask, jewelry, gilded figures and richly inlaid furniture. These items were merely the tip of a "veritable iceberg" of beads, boxes, stools, chariots and much more besides [2]. Examinations were conducted on eight pieces from the shrines at the Royal Botanic Gardens in Kew in 1932 by Dr. C. R. Metcalf to identify their type of wood and as noted by Howard Carter three samples were made of cedar wood and five samples were of sidder wood [3]. Dr. L. Chalk had examined a longish flat piece: "splinter from the shrine and a tongue found in the groove in one of the corners of shrine 207" and their wood type was noted by Howard Carter as Cedar (*Cedrus* sp.) [4]. The shrines were enriched by a layer of thin gold laid on gesso consisting mainly of carbonate of lime [5]. In 2010, some samples from the gilded funerary furniture of Tutankhamun had been identified as imported timbers *Cedrus libani* and *Cupressus sempervirens*. Some of the samples had been covered with a linen textile that had been glued onto the wood and covered by a layer of gesso that consisted of calcite, in addition to some quartz [6]. In 2018, 14 samples of Tutankhamun's small shrines (*naoses*) were analyzed, confirming that Lebanon cedar (*Cedrus libani*) was the most dominant wood species used for making the shrines' body and sleds [7]. In addition to the shrines of Tutankhamen, more than 130 specimens of sticks were found in the tomb from the Antechamber [2]; two of them numbered JE: 61670 - GEM no: 15965 and JE: 61671 - GEM No: 14694 at the Grand Egyptian Museum had also been identified as cedar wood, covered by textile

followed by two preparation layers: coarse gesso overlain by fine gesso [8]. It is worth noting that, in some references-especially in Arabic written Egyptology references- there is a lot of confusion between these two types of wood, as the two words are very similar in transcription and have been translated into the Arabic language in non-botanical references as "*sedr*". Sidder (Ziziphus spina-christi) wood is widely distributed in the Middle East and belongs to Rhamnaceae family, which includes 70 genera and 1500 species of shrubs and small to medium-sized trees [9]. It is a small tree that strongly resists heat and drought [10] and is considered one of the few native tree species that has grown in Egypt since prehistoric times. The tree is characterized by the medicinal value and beneficial effect of all its parts, fruits, leaves and stem extracts that have high content of phenolic compounds, organic and fatty acids, and antioxidants [11]. On the other hand, cedar wood (*Cedrus libani*) is a majestic tree that grows to a height of 15 to 40 m. (49 to 131 feet) at maturity with innumerable scriptural and historical references. It has a thick, massive trunk and wide-spreading branches. When young, it has a pyramidal shape, but as it matures, it develops a flat- topped crown with horizontally tiered branches [12]. Its use dates back to the Predynastic Period, and evidence suggests it was imported into Egypt at an early date [13]. Previous analytical studies on the wood of *Cedrus libani* gave the following results: α-Cellulose 50.2%, hemicellulose 14.3%, and lignin 33.1% [14]. It is described as being pinkish-brown, straight-grained, very durable, takes a good polish and resists rot and insects and has a distinctive scent [15]. In a previous preliminary study, the effect of preparation layers on three native Egyptian wood types (sycamore fig, acacia and Tamarix) was conducted using FTIR, SEM and SEM-EDX [16,17]. In this study the work will be continued on two other types of wood and four preparation layers simulating some of the preparatory layers of Tutankhamun's collection. The objective is to investigate and assess the changes occurring between preparation layers and the chemical composition of two types of wood commonly used in ancient Egypt, namely cedar wood (*Cedrus libani*) and sidder (*Ziziphus spina-christi*). These are two of many types of wood which have been identified in Tutankhamun's collection as aforementioned and are rich in different types of extractives. The analyses here are conducted using FTIR and ATR-FTIR mapping, and the results of both analytical techniques are discussed and compared.

2. Materials and Methods

2.1. *Sacrificial wooden samples*

A softwood and a hardwood, Lebanese cedar and sidder, respectively, were chosen for this experimental study. These two types of wood had been identified in the collection of Tutankhamun. Lebanese cedar wood was imported from Lebanon for this study, while sidder wood is a local hardwood came from Giza, Egypt. Six blocks of each type of wood were cut into (3×3×3 cm) cubes, which comprised of one control sample before accelerated aging, one sample after heat aging without preparation layers and four samples covered with preparation layers that had been added to the heat aged wood.

2.2. *Preparation layers*

Experimental wood blocks were covered with gesso layers similar to those found in artifacts dating back to the New Kingdom, especially on the wood identified from the tomb of Tutankhamun. Calcium carbonate was a main component, in addition to some gypsum in some cases. Gesso was applied to wood as a white preparation ground for painting and gilding techniques and there was sometimes a layer of coarse woven fabric (linen) between the two; where the canvas was probably treated with glue to make it adhere to the wood on one side and to the plaster on the other side [13]. In this study the four preparation layers used as a thin layer contained limestone powder ($CaCO_3$) [18], hemi hydrated gypsum or plaster of Paris ($CaSO_4.^1/_2H_2O$) [19] which turned into hydrated gypsum ($CaSO_4.2H_2O$) by mixing it with water and hide glue. Gypsum was from Sina GIPS Company, Giza, Egypt. Calcium carbonate was prepared from grinding limestone at the Conservation dept., Faculty of Archaeology, Cairo Univ. Each wood block was covered separately, fig. (1) as follows: ***)** Calcium carbonate (chalk) + water. ***)** Calcium carbonate (chalk) + hide glue solution (1glue:15 water v/v). ***)** Calcium carbonate (chalk) 30 g + gypsum 4.5g +hide glue solution (1glue:15 water v/v) after priming the wood surface with hide glue. ***)** Calcium carbonate (chalk) 30 g +gypsum 4.5 g + hide glue solution (1glue:15 water v/v) after covering the wood surface with a layer of glued unbleached linen textile.

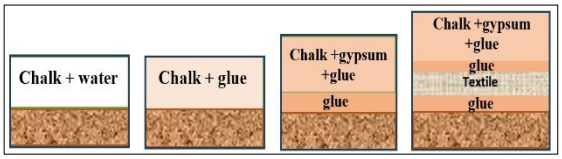

Figure (1) the stratigraphy of the preparation layers that covered each wood block.

2.3. *Aging process*

Wooden samples were exposed to accelerated aging procedures to assess the long-term degradation processes over a short period of time at the National Institute of Standards. All samples were exposed to dry-heat aging at 90ºC [20,21] for 120 hours.

2.4. *pH measurements*

pH measurements of all preparation layers were conducted using a pH meter, model; ADWA Kft, at the Conservation dept., Faculty of Archaeology, Cairo Univ.

2.5. *Digital microscope examination*

The cross sections of the samples were investigated using a digital microscope, XVZ, Model; USB X4, 500X to 1600X optical zoom; and the calcium carbonate crystals were obvious at a magnification from 500-X to 1600-X.

2.6 *Analytical methods*

During the five days of heat-aging process, the preparation layers partially separated from the wood, especially (Chalk-water) samples in both types of wood. However, in sidder samples, all layers separated except the textile sample remained stable, making it easier to analyze their surfaces. Lebanese cedar samples' preparation layers remained stable. The stable-attached preparation layers of Lebanese cedar and sidder textile sample were carefully removed using a scalpel without scratching the samples' surfaces after aging process and the wood that lay directly beneath the layer was examined and analyzed.

2.6.1. Fourier transform infra-red spectroscopy (FTIR)

FTIR analyses were conducted using a Nicolet 380 spectrometer with high-performance DTGS detector mounted on pre-aligned, pinned-in-place baseplate for optimal sensitivity at the National Institute of Standards, Giza, Egypt. The wavenumber range was 4000-400 cm^{-1}, in transmission mode using KBr pellet technique (0.02 gm of KBr was added to each of the samples) at lab temperature 20°C and 65 % RH. Peak heights and width of absorption bands were measured by Essential FTIR software (version 350.218) and Excel. Lignin/Carbohydrate ratios were calculated according to El Hadidi [22].

2.6.2. Attenuated total reflectance-fourier transform infrared spectroscopy (ATR-FTIR mapping)

ATR-FTIR analysis were conducted using attenuated total reflection—fourier transform infrared spectroscopy (ATR-FTIR, Alpha Bruker platinum, 1-211-6353) at the Applied Research Institute for Petroleum Research, Cairo, Egypt, using a zinc selenide crystal with an incident angle of 45±15 ° and 560 scan time at 4 cm^{-1} resolution. The wavenumber range was 4000-600 cm^{-1}, in transmission mode. Peak heights and width of absorption bands were measured by Essential FTIR software (version 350.218) and Excel. FTIR Microscopy Analysis has been performed on the cross-sections of all the samples which were cut into (0.5×0.5×0.5 cm) cubes and separated from the experimental wood blocks for mapping using the LUMOS fully motorized stand-alone FTIR microscope in ATR mode (Bruker Optik GmbH Ettlingen, Germany). ATR-FTIR analyses focused on a square of 25 spots (50-µ spacing) and linearly on 5 spots separated by 2-µ spacing, contrary to FTIR chemical images, where a single-point analyses is conducted in selected areas as shown in fig. (2), The magenta and the blue false colors in FTIR Mapping denote high and low absorbance [23]. ATR-FTIR data and images were evaluated using the OPUS software (Bruker, Germany).

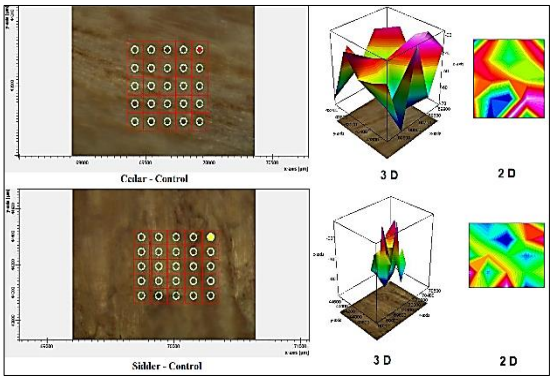

Figure (2) Cedar and sidder wood control samples after focusing on a square area with a length of 5 points on every side which equals 25 points for ATR-FTIR mapping images and the 2D and 3D images of one point in each sample.

3. Results

3.1. *pH measurements*

pH of preparation layers' solutions was measured according to the developed method of standard STN 50 0374 for testing pulp and paper in the cold-water extract method [24] at lab temperatures between 21°C and 22° C, and results ranged between 7.2 and 7.5 as follows: ***)** Chalk and water (0.5 g calcium carbonate + 10 ml distilled water), pH 7.5. ***)** Chalk and glue (0.5 g calcium carbonate + 10 ml glue solution, pH 7.2. ***)** Chalk + gypsum + glue (0.5 g calcium carbonate + small portion of gypsum+10 ml glue solution), pH 7.3

3.2. *Digital microscope results*

Lebanese cedar is a non-porous wood (softwood), in the transverse section of the control sample the gradual transition from earlywood wide-thin cells to latewood narrower-thick cells were evident, fig. (3-a). In the transverse section of the sidder control samples diffuse, solitary or multiples vessels of 2 in small clusters were clearly noted and there is no clear distinction between earlywood and latewood, fig. (3-b). In the transverse section of the Lebanese cedar wood samples, chalk-water based preparation layers showed calcium carbonate crystals in a dry form on the tracheids in earlywood and latewood, fig. (4-a). In chalk-glue based preparation layers, calcium carbonate crystals appeared along the length of tracheid's cell walls and the high viscosity of glue on latewood

cell walls is clearly seen, fig. (4-b), whereas in chalk-gypsum and glue-based preparation layers wide layers of calcium carbonate and gypsum covered the wood's cell walls, fig. (4-c). The chalk and gypsum-based preparation layers above the linen textile layer showing calcium carbonate and gypsum layer covered some tracheids, but in other areas no crystals of preparation layer were seen, which is due to the linen textile layer which worked as a filtration layer above the wood cells, fig. (4-d). In the transverse section of sidder samples, chalk-water based preparation layers showed calcium carbonate crystals on wood vessels, fig. (5-a). In chalk-glue based preparation layers, calcium carbonate crystals mixed with glue appeared along the transverse section hiding wood fibers and vessels as in the case of Lebanese cedar, fig. (5-b), but in the case of the chalk-gypsum and glue-based preparation layers calcium carbonate crystals around the circular edges of some vessels are present, fig. (5-c). Chalk and gypsum-based preparation layers on the linen textile layer, showed calcium carbonate crystals around circular edges of some solitary and multiples vessels but other areas appeared with no crystals of preparation layer again due to the linen textile layer which worked as a filtration layer above the wood cells, fig. (5-d).

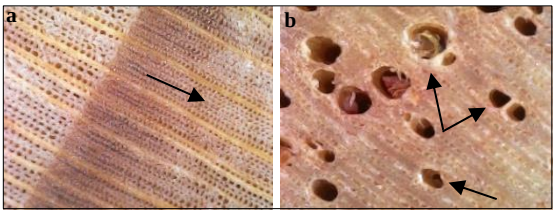

Figure (3) transverse sections of the control samples of Lebanese cedar and sidder wood; **a.** arrow showing gradual transition from early wood to latewood in Lebanese cedar, **b.** arrows showing diffuse vessels, solitary or in small clusters of 2 vessels in sidder wood.

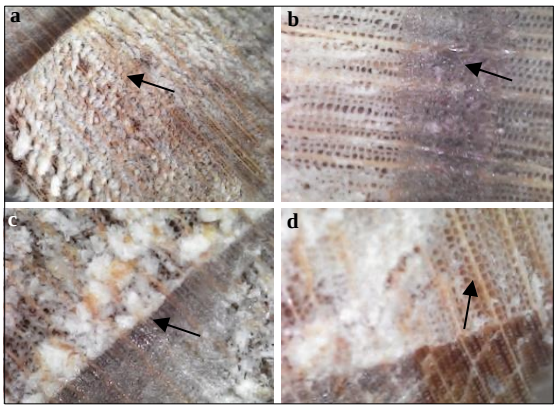

Figure (4) transverse sections of Lebanese cedar treated samples; **a.** chalk-water based preparation layer, arrow delimit calcium carbonate crystals, **b.** chalk-glue based preparation layer, arrow delimit the viscosity appearance of glue, **c.** chalk and gypsum-glue preparation layer, arrow delimit chalk and gypsum layer on wood cells, **d.** textile and chalk+gypsum+glue-based preparation layer, arrow delimit the unaffected wood area with preparation layer.

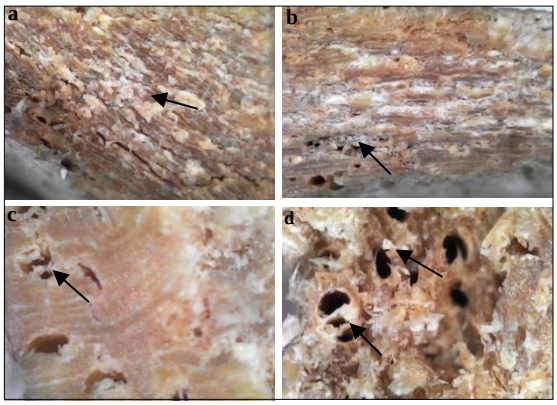

Figure (5) transverse sections of sidder treated samples; **a.** chalk-water based preparation layer, **b.** chalk-glue based preparation layer, **c.** chalk and gypsum-glue preparation layer, **d.** textile and chalk+gypsum+glue-based preparation layer, arrow de limit calcium carbonate crystals above multiples vessels.

3.3. *FTIR and FTIR-ATR mapping*

FTIR and ATR-FTIR results were recorded in each type of wood according to Pandey 1999, Fickler 2010 and Chen 2015 [25-27] and calcium carbonate bands were recorded according to Chen 2010 and Yao 2013 [28,29]. In the single-point analyses, which were followed by FTIR chemical images, the chemical images data sets were integrated for the ranges between (800-900 cm^{-1}), (1370-1380 cm^{-1}) and (1420-1430 cm^{-1}) which are assignable to cellulose. The range between (1730-1740 cm^{-1}) is assignable to hemicellulose and the range between (1505-1513 cm^{-1}) is assignable to lignin. The color scale from blue to pink indicates increase of intensities; the corresponding chemical images of Lebanese cedar and sidder.

3.3.1. Carbohydrate and lignin bands in Lebanese cedar and sidder in FTIR, FTIR-ATR spectra and FTIR mapping

There were slight differences between all bands of cellulose, hemicellulose and lignin which were present in the two types of wood as recorded in tab$_s$. (1 & 2) and fig. (6) In this study the main bands that were compared are as follows:

3.3.1.1. *Cellulose bands*

Cellulose bands in both types of wood were at around 1427 cm^{-1}, 1375cm^{-1}, 1335 cm^{-1}, 1165 cm^{-1} and 898 cm^{-1} with high transmittance in Lebanese cedar wood and low transmittance in sidder wood.

3.3.1.2. *Hemicellulose bands*

Hemicellulose bands at 1735 cm^{-1} and 1061 cm^{-1} were found in the two types of wood with higher transmittance in Lebanese cedar wood than sidder wood.

3.3.1.3. *Lignin bands*

According to literature lignin bands are found at 1505-1513 cm^{-1} with higher intensity in softwood than hardwood, and that was evident in Lebanese cedar wood which had a lignin band at 1510 cm^{-1}

with higher intensity than sidder wood at 1508 cm^{-1}. The bands at around 1595-1605 cm^{-1} were absent in both wood types.

3.3.2. Carbohydrate and lignin bands in heat-aged Lebanese cedar and sidder wood after application of different preparation layers using FTIR and ATR-FTIR mapping

3.3.2.1. *Heat-aged samples*

➢ **FTIR**

The effect of heat was evident in both types of wood. The OH area at 3448 cm^{-1} in the aged sample became narrower than the control sample with a 6 cm^{-1} shift in Lebanese cedar wood, while in sidder wood this band remained relatively stable in comparison to the control sample with a 2 cm^{-1} shift. The H-O-H area at 1635 cm^{-1} in the aged sample became narrower than the control sample with a 1 cm^{-1} shift in Lebanese cedar wood and in sidder wood this band became slightly wider than the control sample with a 1 cm^{-1} shift. Lignin band in the cedar wood remained stable after exposure to heat in comparison to the control sample at 1511 cm^{-1} and in sidder wood the lignin band became slightly wider at 1509 cm^{-1} with a 1 cm^{-1} shift compared with the control wood sample. Cellulose bands at 1427 cm^{-1}, 1379 cm^{-1}, 896 cm^{-1} in the aged samples remained stable, while a 1 and 3 cm^{-1} shift occurred in the bands at 1322 cm^{-1}, 1159 cm^{-1}, respectively. Hemicellulose band at 1737 cm^{-1} became weaker with a 7 cm^{-1} shift after aging in comparison to the control sample. On the contrary, cellulose and hemicellulose bands in sidder wood showed stronger transmittance with a 1 cm^{-1} shift after aging in comparison to the control sample at 1737 cm^{-1}, 1380 cm^{-1}, 1330 cm^{-1}, and a 2 cm^{-1} shift at 1427 cm^{-1} and 897 cm^{-1}, while and the band at 1159 cm^{-1} became slightly weak with a 2 cm^{-1} shift.

➢ **ATR**

In Lebanese cedar cellulose, hemicellulose and lignin bands appeared in the aged sample except the band at 1149 cm^{-1} that did not appear in the control sample. In sidder wood all wood bands appeared except the bands at 1370 cm^{-1} and 1100 cm^{-1}. In Lebanese cedar and sidder wood the OH bands appeared in the control samples at more than one peak and in the aged samples at one peak only.

Table (1) comparison between FTIR and FTIR-ATR bands in Lebanese cedar wood.

Wood				Chalk, Water		Chalk glue		Chalk, Gypsum, Glue		Textile, Chalk Gypsum, Glue		Assigned Bands
Before ageing		*After ageing*										
FTIR	*ATR*	*FTIR*	*ATR*	*FTIR*	*ATR*	*FTIR*	*ATR*	*FTIR*	*ATR*	*FTIR*	*ATR*	
3448	3380 3311 3277	3454	3346	3456	3384 3278	3452	3389 3280	3458	3423 3356	3460	3383 3334 3288	H stretching absorption around (3300-3400cm^{-1}) [30]–O
2924	2917 2881	2924	2900	2928	2920 2873	2929	2917 2883	2926	2930 2881 2836	2929	2944 2881	C–H stretching absorption around (2800-3000cm^{-1}) [30-32]
1737	1732	1730	1729	1728	1730	1738	1739	1730	1744 1708	1738	1729	unconjugated C = O in xylans (1735-1740 cm^{-1}) [33]
1635	1646 1610	1636	1647	1645	1642 1604	1645	1687 1641	1636	1663 1629	1644	1666 1621	Conjugated C=O stretching H-O–H in cellulose (1610-1640 cm^{-1}) [30,33,34]
1551 1511	1554 1510	1554 1511	1598 1566 1504	1552 1513	1535	1511	1582	1510	1581	1552 1512	1508	C=C stretching vibration in aromatic ring in lignin aromatic skeletal (1505-1605cm^{-1}) [33]
1460 1427	1416	1460 1426	1450 1421	1460 1427	1419	1459 1426	1402	1485 1427	1411	1458 1427	1408	C–H deformation in lignin and carbohydrates (1420-1430 cm^{-1}) [35] symmetric stretching and asymmetric stretching of CO_3^{-2} group at about 1080 and 1400 cm^{-1} [28]
1379	1366	1379	1367	1381		1381		1381		1382		C–H deformation in cellulose and hemicelluloses (1346-1384 cm^{-1}) [36]
1322	1319	1323	1321	1321	1321	1321		1323		1338		C–H vibration in cellulose and C1–O vibration in syringyl derivatives (1315-1330 cm^{-1}) [25]
1268	1263	1269	1264	1269	1261	1269		1269	1266	1269		C–O stretch in lignin and C–O linkage in guaiacyl aromatic methoxyl groups (1265-1275 cm^{-1}) [37,38]
1233	1224	1229		1230	1218							syringyl ring and C–O stretch in lignin and xylans (1220-1230cm^{-1}) [39]
1159	Absent	1156	1149	1156		1156	1172 1145	1157	1148	1157	1152	C–O–C stretch in cellulose (1150-1160cm^{-1}) [40]
1061	1031	1062	1036	1068	1032	1061	1045	1067	1100 1020	1064	1030	C–O stretch in cellulose and hemicellulose (1060-1117 cm^{-1}) [40]
896	897	896	888	896		896	948	895	951		946	C–H deformation in cellulose [33]
871				876	873	876	870	875	874	875	872	CO_3^{-2} group [28,29,41] C–H out-of-plane bending mode [42]

Table (2) comparison between FTIR and FTIR-ATR bands in Sidder wood.

Wood				Chalk, Water		Chalk glue		Chalk, Gypsum Glue		Textile, Chalk Gypsum, Glue		Assigned Bands
Before ageing		*After ageing*										
FTIR	*ATR*	*FTIR*	*ATR*	*FTIR*	*ATR*	*FTIR*	*ATR*	*FTIR*	*ATR*	*FTIR*	*ATR*	
3450	3412 3360 3321	3452	3375	3459	3401 3357 3315	3456	3405 3352 3313	3452	3397 3356 3313	3448	3388 3353 3309	H stretching absorption around (3300-3400 cm^{-1}) [30]–O
2924	2936 2877	2929	2916	2936	2924 2876	2938	2918 2882	2928	2919	2924	2920 2838	C–H stretching absorption around (2800-3000cm^{-1}) [30-32]

1737	1728	1738	1727	1739	1733	1739	1712	1739	1727	1732		unconjugated C = O in xylans (1735-1740 cm^{-1}) [33]
1635	1673	1636	1660	1636	1644	1645	1649	1645	1648	1636	1658	H in cellulose (1610-1640 –O-Conjugated C=O stretching H
	1618		1627		1602		1601		1616		1628	cm^{-1}) [30,33,34]
1509	1546	1552	1566	1551	1506	1550		1552		1552		C=C stretching vibration in aromatic ring in lignin aromatic
	1505	1510	1516	1511		1510		1510		1506		skeletal (1505-1605cm^{-1}) [33]
1461	1456	1462	1450	1463	1423	1462	1406	1462	1410	1458	1409	C–H deformation in lignin and carbohydrates (1420-1430 cm^{-1})
1427	1414	1425	1422	1427		1427		1426		1426		[35] symmetric stretching and asymmetric stretching of CO_3^{-2}
												group at about 1080 and 1400 cm^{-1} [28]
1380		1379		1382	1368	1387		1381		1383		C–H deformation in cellulose and hemicelluloses (1346-1384 cm^{-1}) [36]
1330	1322	1329	1325	1332	1318	1338		1330		1334		C–H vibration in cellulose and C1–O vibration in syringyl
												derivatives (1315-1330 cm^{-1}) [25]
1263	1232	1263	1238	1264	1236	1265	1239	1262	1257	1263		C–O stretch in lignin and C–O linkage in guaiacyl aromatic
												methoxyl groups (1265-1275 cm^{-1}) [37, 38]
1159	Absent	1157		1156		1159		1156	1147	1156	1145	C–O–C stretch in cellulose (1150-1160cm^{-1}) [40]
1115	1035	1059	1032	1070	1030	1117	1033	1061	1097	1120	1100	C–O stretch in cellulose and hemicellulose (1060-1117 cm^{-1}) [40]
1061						1059			1036	1060		
897	902	897	894	897		897	913	897	915		925	C–H deformation in cellulose [33]
	825											
			818		885	876	873		872	875	874	CO_3^{-2} group [28,29,41] C–H out-of-plane bending mode [42]

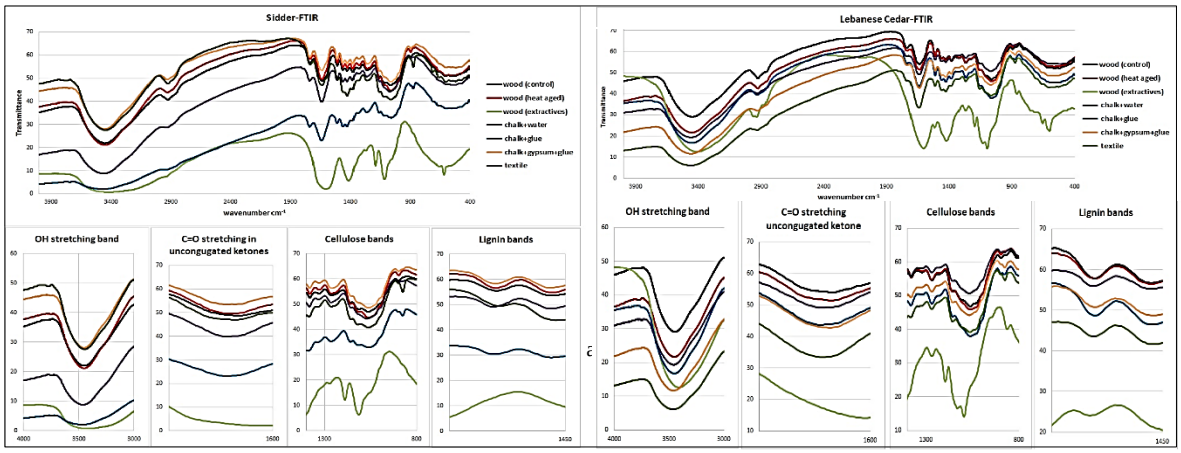

Figure (6) FTIR analysis of Lebanese cedar wood and sidder wood after ageing and after application of all preparation layers on both types of wood separately.

3.3.2.2. *The effect of chalk-water based preparation layers on wood*

➢ **FTIR**

The effect of chalk, which was slightly alkaline, was evident in both types of wood. Lignin bands in the cedar wood became narrower after the treatment in comparison to the control sample at 1511 cm^{-1} with a 2 cm^{-1} shift and in sidder wood lignin bands became narrower at 1509 cm^{-1} with a 1 cm^{-1} shift compared with the control sample. Cellulose bands in the treated samples became wider than the control sample at 1379 cm^{-1}, 1322 cm^{-1}, 1159 cm^{-1} and 896 cm^{-1} and the band at 1427cm^{-1} became relatively narrow after treatment. Hemicellulose band at 1737 cm^{-1} became narrower with a 9 cm^{-1} shift after treatment in comparison to the control sample. On the contrary cellulose and hemicellulose bands in sidder wood showed narrower transmittance after treatment in comparison to the control sample at 1737 cm^{-1}, 1380 cm^{-1}, 1330cm^{-1}, 1159cm^{-1}, 1427 cm^{-1} and at 897cm^{-1}.

➢ **ATR**

In Lebanese cedar cellulose, hemicellulose and lignin bands had a small transmittance and some of them did not appear. At 1730 cm^{-1} and 1032 cm^{-1} bands in hemicellulose had low intensity in comparison to the untreated sample. Cellulose bands only appeared at 1419 cm^{-1}, 1321 cm^{-1} and at 1032 cm^{-1}. Lignin band appeared only at 1535 cm^{-1} after treatment. Calcium carbonate band appeared after treatment at 873 cm^{-1}. In sidder wood all wood bands had low intensities; cellulose bands appeared at 1423 cm^{-1}, 1368 cm^{-1} and 1318 cm^{-1}, hemicellulose bands appeared at 1733 cm^{-1} and 1030 cm^{-1} and the lignin band appeared at 1506 cm^{-1}. Calcium carbonate band appeared after treatment at 885cm^{-1}.

3.3.2.3. *The effect of chalk-animal glue-based preparation layers on wood*

➢ **FTIR**

The FTIR spectra in Lebanese cedar and sidder wood indicated that all cellulose, hemicellulose and lignin bands were affected by this treatment. In comparison to chalk-water based preparation samples all bands became narrower after the treatment by chalk-animal glue-based preparation layers. In Lebanese cedar wood cellulose bands at 1427 cm^{-1} became narrower with a 1 cm^{-1} shift, 1379 cm^{-1} band became narrow with a 2 cm^{-1} shift, 1322 cm^{-1} band had a weak transmittance only, 1159 cm^{-1} weakened with

a 3 cm^{-1} shift and 896 cm^{-1} band had a small intensity. Hemicellulose bands at 1737 cm^{-1} and 1060 cm^{-1} showed weak transmittance after treatment. Lignin band at 1511 cm^{-1} became narrower in comparison to the control sample. In sidder wood; cellulose bands at 1427 cm^{-1}, 1159 cm^{-1}, 897 cm^{-1} became small, 1380 cm^{-1} band became narrow with a 7 cm^{-1} shift and 1330 cm^{-1} band had a weak transmittance with an 8 cm^{-1} shift. Hemicellulose bands at 1737 cm^{-1} and 1060 cm^{-1} showed weak transmittance after treatment with a 2 cm^{-1} shift. Lignin band at 1509 cm^{-1} became weaker with a 3 cm^{-1} shift in comparison to the control sample.

➢ **ATR**

In both Lebanese cedar and sidder the cellulose bands did not appear. Hemicellulose and lignin bands had a strong transmittance after treatment at 1739 cm^{-1}, 1045 cm^{-1}, 1582 cm^{-1} and calcium carbonate bands appeared after treatment at 1402 cm^{-1} and at 870 cm^{-1} in the case of Lebanese cedar. In sidder wood hemicellulose bands had a strong transmittance after treatment at 1712 cm^{-1} and 1033 cm^{-1} and lignin band disappeared at 1505 cm^{-1}. Calcium carbonate bands appeared clearly after treatment at 1406 cm^{-1} and at 873 cm^{-1}.

3.3.2.4. *The effect of chalk and gypsum-based preparation layers on wood*

➢ **FTIR**

Priming wood by animal glue before preparation layers may act as a protective layer which lessens the effect of chalk and gypsum on sidder wood. All sidder wood bands of cellulose, hemicellulose and lignin had strong intensities after treatment. Lebanese cedar wood showed different results; all cellulose and lignin bands had weak intensities and hemicellulose bands at 1730 cm^{-1} decreased. These results are the complete opposite to the effect of chalk-water based preparation layers on the two types of wood.

➢ **ATR**

In Lebanese cedar wood; cellulose bands disappeared and some of them had small transmittance, hemicellulose and lignin bands decreased after treatment at 1744 cm^{-1}, 1708 cm^{-1}, 1100 cm^{-1} and 1581 cm^{-1} and calcium carbonate bands appeared after treatment at 874 cm^{-1}. In sidder wood; cellulose bands did not appear, except for the band at 1147 cm^{-1}, hemicellulose bands had a strong transmittance after treatment at 1727 cm^{-1} and 1097 cm^{-1} and lignin band disappeared at 1505 cm^{-1}. Calcium carbonate bands appeared clearly after treatment at 1410 cm^{-1} and 872 cm^{-1}.

3.3.2.5. *The effect of chalk and gypsum-based preparation layers above the linen textile layer on wood*

➢ **FTIR**

In Lebanese cedar cellulose bands at 1379 cm^{-1}, 1322 cm^{-1}, 1159 cm^{-1} decreased with shifts, 1427 cm^{-1} band became small and 896 cm^{-1} band disappeared. Hemicellulose bands at 1737 cm^{-1} and 1061 cm^{-1} decreased. Lignin band at 1511 cm^{-1} became weaker with a 2 cm^{-1} shift. In sidder wood cellulose bands at 1380 cm^{-1}, 1330 cm^{-1}, 1159 cm^{-1} decreased with shifts, 1427 cm^{-1} band became small and 897 cm^{-1} band also disappeared. Hemicellulose bands at 1737 cm^{-1} and 1061 cm^{-1} decreased with shifts. Lignin band at 1509 cm^{-1} became weaker with a 3 cm^{-1} shift.

➢ **ATR**

In Lebanese cedar wood; cellulose bands disappeared despite the band at 1152 cm^{-1}, hemicellulose and lignin bands increased after treatment at 1729 cm^{-1}, 1030 $cm^{-1}$and 1508 cm^{-1} and calcium carbonate bands appeared after treatment at 1408 cm^{-1} and at 872 cm^{-1}. In sidder wood cellulose bands, hemicellulose and lignin bands disappeared after treatment except for the bands at 1145 cm^{-1} and 1100 cm^{-1}. Calcium carbonate bands appeared clearly after treatment at 1409 cm^{-1} and 874 cm^{-1}.

3.3.3. Comparison between FTIR analysis and FTIR mapping in Lebanese cedar and sidder wood

3.3.3.1. *Lebanese cedar samples*

By comparing FTIR spectra of Lebanese cedar with FTIR-mapping chemical images, it could be asserted that the area between 1505-1513 cm^{-1} had the highest intensity in the chalk-glue sample and showed the highest lignin content compared to other samples' images in this area, which is identical with FTIR-mapping image of the same sample. The lowest intensity appeared in chalk-water sample and textile+ chalk+gypsum+glue sample which agrees with FTIR-mapping images in the lignin area at 1505-1513 cm^{-1}. The area between 1735-1740 cm^{-1} had the highest intensity in Lebanese cedar control sample and that is again in agreeance with the FTIR-mapping image in the sample, in which part of cell wall was red in color. The lowest intensity appeared in chalk+gypsum+glue sample which is consistent with FTIR-mapping image which showed small portions of cell walls in orange-red color in the hemi-cellulose area at 1735-1740 cm^{-1}. The area between 1420-1430 cm^{-1} had the highest intensity in chalk-glue sample, and that is in agreeance with ATR-FTIR-mapping image, which showed high cellulose content evenly distributed in the cell walls. The lowest intensity appeared in textile+chalk+gypsum+ glue sample which is also consistent with FTIR-mapping image, where uneven distribution of cellulose in the cell wall in the area at 1420-1430 cm^{-1} was recorded. The area between 1370-1380 cm^{-1} had the highest intensity in the control sample and chalk-glue sample and corresponds with FTIR-mapping images in these samples which showed high cellulose content evenly distributed in the cell walls. The lowest intensity appeared in chalk+gypsum+glue sample, which also agrees

with FTIR-mapping image which showed uneven distribution of cellulose in the cell wall in the area at 1370-1380 cm^{-1}. The area between 890-900 cm^{-1} had the highest intensity in the aged sample and the control sample and that is in agreeance with FTIR-mapping images in the control sample which showed intense distribution in the cell wall layers. The lowest intensity appeared in chalk+gypsum+glue sample and textile+chalk+gy-psum+ glue sample which also agrees with FTIR-mapping image in the textile sample, which showed small percentages in some parts of the cell wall in the area at 890-900 cm^{-1}.

3-3-3-2 Sidder samples

On the contrary to the Lebanese cedar samples, there are many differences between the FTIR intensities of sidder bands and the chemical images in ATR-FTIR-mapping. The area between 1735-1740 cm^{-1} had the highest intensity in chalk-water sample and that is not in agreement with FTIR-mapping image of the same sample, in which the middle lamella and parts of the cell wall were in orange color. The lowest intensity appeared in chalk-glue sample, which also did not match the FTIR-mapping image, which showed red-orange color in parts of the cell wall and middle lamella in hemicellulose area at 1735-1740 cm^{-1}. The area between 1505-1513 cm^{-1} had the highest intensity in both the aged sample and the control sample, which were in agreeance with the FTIR-mapping image in the control sample that showed high lignin content in the middle lamella only. The lowest intensity appeared in textile+chalk+gypsum+glue sample, which was also in agreeance with FTIR-mapping image in the lignin area at 1505-1513 cm^{-1}. The area between 1420-1430 cm^{-1} had the highest intensity in textile+chalk+gypsum+glue sample, which totally corresponded with the FTIR-mapping image in the sample that showed extremely high distribution of cellulose in the cell wall. The lowest intensity appeared in the control sample which matched with FTIR-mapping image that showed uneven distribution of carbohydrates in the cell wall in the area at 1420-1430 cm^{-1}. The area between 1370-1380 cm^{-1} had the highest intensity in chalk-water sample, which did not agree with FTIR-mapping image in this sample that showed even distribution of cellulose in the cell wall. The lowest intensity appeared in textile+chalk+gypsum+glue sample, which is also not in agreeance with FTIR-mapping image that showed very high cellulose content in parts of the cell walls in the area at 1370-1380 cm^{-1}. The area between 890-900 cm^{-1} had the highest intensity in chalk+glue sample, and that did not match the FTIR-mapping image, which showed weak percentage in the middle lamella. The lowest intensity appeared in chalk-water sample which is also not in correspondence with FTIR-mapping image which showed small amount in the cell wall layers in the area at 890-900 cm^{-1}, but the control sample had a very small amount in the cell wall layers. All the aforementioned results are summarized in tab. (3) and figs. (7 & 8).

Table (3) changes in peak heights in FTIR spectra of Lebanese cedar and sidder after aging (in comparison to the control samples) and after addition of preparation layers (in comparison to the aged wood samples).

	Wood after ageing	Chalk+water	Chalk+glue	Chalk+gypsum+glue	Textile
Lebanes	All lignin and carbohydrates bands decreased	All lignin and carbohydrates bands decreased	Lignin, hemicellulose and cellulose bands decreased except the cellulose band at 896 cm^{-1}	Lignin, hemicellulose, and cellulose bands decreased except the cellulose band at 1427 cm^{-1} which had a slight increase.	All lignin and carbohydrates bands decreased except the cellulose band at 1159 cm^{-1}
Sidder	All lignin and carbohydrates bands increased except the band at 1375 cm^{-1}	All lignin and carbohydrate bands increased except bands at 1511 cm^{-1} and 897 cm^{-1}	Lignin, hemicellulose, and cellulose bands decreased except the cellulose bands at 897 cm^{-1}, 1159 cm^{-1} and 1427 cm^{-1}	All bands increased except the bands at 1159 cm^{-1} and 1511 cm^{-1}	All bands increased except the lignin band at 1506 cm^{-1} and the band at 1383 cm^{-1}

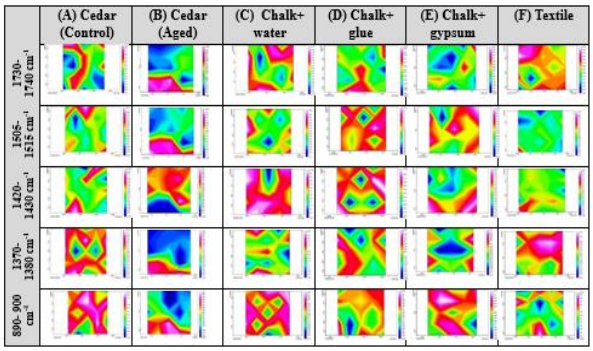

Figure (7) FTIR-ATR Mapping of Lebanese cedar samples

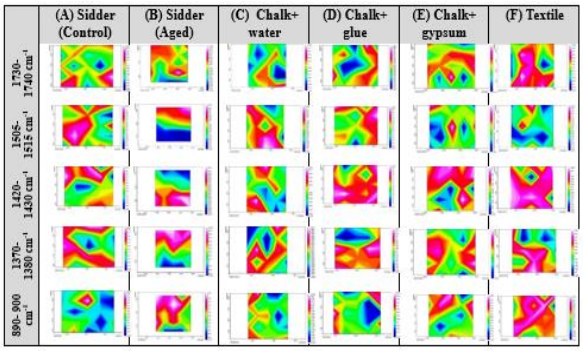

Figure (8) FTIR-ATR Mapping of sidder samples

3.3.4. Comparison between carbohydrate/lignin ratios in Lebanese cedar and sidder wood in FTIR analysis, figs. (9 & 10)

All Lebanese cedar wood samples in comparison to the control sample proved that all carbohydrate to lignin ratios decreased except for the band at 897 cm^{-1} in the aged sample. Chalk+water sample had low carbo-hydrate to lignin ratios except the bands at 1427 cm^{-1} and 1156 cm^{-1}. Chalk+glue sample had weak carbohydrate to lignin ratios. In chalk+gypsum+

glue sample, carbohydrate to lignin ratios decreased except those bands at 1425 cm^{-1} and 1156 cm^{-1}. Textile+Chalk+ gypsum+glue sample had weak carbohydrate to lignin ratios except for the band at 1156 cm^{-1}. Within the same context, sidder wood samples in comparison to the control sample, affirmed that all carbohydrate to lignin ratios decreased except the band at 1375 cm^{-1} in the aged sample. Chalk+ water sample had high carbohydrate to lignin ratios except the bands at 897 cm^{-1} and 1156 cm^{-1}. Chalk+glue sample had high carbohydrate to lignin ratios except the bands at 1375 cm^{-1} and 1735 cm^{-1}. In chalk+ gypsum+glue sam-ple, carbohydrate to lignin ratios increased. Textile+ Chalk+gypsum+glue sample had high carbohydrate to lignin ratios except the band at 1375 cm^{-1}.

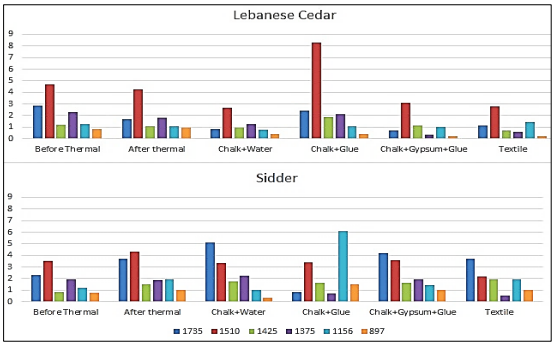

Figure (9) Carbohydrate/Lignin intensities in Lebanese cedar and sidder samples, before and after thermal ageing and covered with different preparation layers

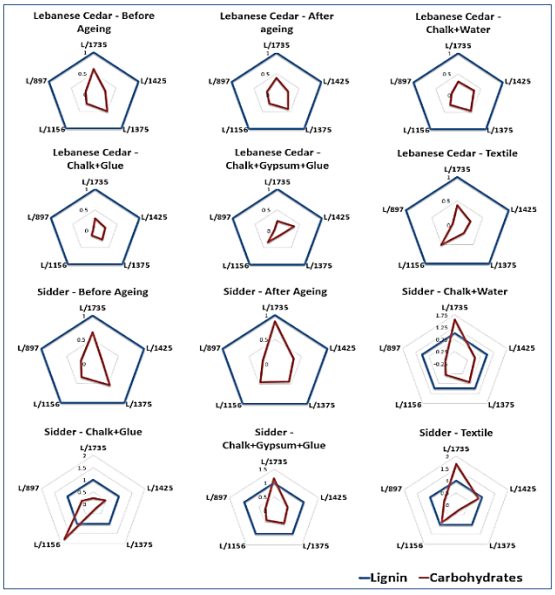

Figure (10) Carbohydrate/Lignin ratios of cedar and sidder samples

4. Discussion

Generally, softwood has a higher content of carbohydrates and lignin than hardwood, according to Unger 2001 [43] and that was obvious in both FTIR and ATR-FTIR analysis of the two untreated wood samples. Carbohydrates and lignin bands of Lebanese cedar wood have relatively higher intensities than sidder wood bands. In FTIR analysis, all wood bands were clear and sharp in both high and low transmittances. In the aged samples, the effect of heat was noticeable in Lebanese cedar and sidder wood, all OH bands and (H-O-H) bands were affected due to the oxidation process and there was a slight effect on cellulose, hemicellulose and lignin bands. In the samples covered with chalk-water based preparation layers, the low alkaline effect was noted in Lebanese cedar wood as lignin bands decreased and some of the carbohydrate bands were affected. However, in sidder wood samples, all wood bands were affected by this treatment. In the samples covered with chalk-glue-based preparation layers, all wood bands in both wood types were affected, and a probable explanation of this might be because wood samples were not covered by a layer of glue before applying preparation layers which led to higher absorbance of chalk and glue. In the case of the samples that were covered with chalk and gypsum-glue-based preparation layers, in which priming of wood was applied using animal glue before adding the preparation layers, the animal glue worked as a protective layer which lessened the effect of chalk and gypsum in sidder wood, on the contrary to Lebanese cedar wood, where all wood bands decreased after treatment and that might be because of the difference between Lebanese cedar wood and sidder wood density and porosity. Samples covered with chalk and gypsum-based preparation layers above a linen textile layer, showed that all lignin and carbohydrates bands decreased and cellulose band at 890 cm^{-1} disappeared in both Lebanese cedar wood and sidder wood which may be due to the dual effect of chalk and gypsum together. However, ATR-FTIR analysis gave different results which were not always compatible with FTIR analysis at some points. In ATR-FTIR analysis, wood bands disappeared in some cases and had different transmittance despite of the presence of chalk. Chalk bands at 1405 cm^{-1} and 873 cm^{-1} appeared clearly in ATR-FTIR analysis, but some of the lignin and carbohydrates bands disappeared or decreased while some gave strong transmittance values. In ATR-FTIR mapping images, where single-point analysis was used in each wood sample, different results in comparison to FTIR analysis and ATR-FTIR analysis were obtained. However, when comparing carbohydrates/lignin ratios from FTIR analysis in each type of wood to FTIR chemical images, similarities were observed in both results. In FTIR analysis, samples were prepared in the form of KBr pellets mixed with the sample in the form of a powder, the results are clear and can be correlated to each other. In ATR-FTIR analysis,

samples were prepared in the form of a 0.5 cm thick square and the focus in the analysis was on a square area with a length of 5 points to every side equaling 25 points for each sample. However, in the chemical images, the focus was on one single-point analysis. This explains why the results were different from one technique to the other due to the anisotropic and inhomogeneous properties of the samples. The chemical distribution of wood components appeared clearly in ATR-FTIR chemical images. The portions of cell walls and cell lumens were different in all images, leading to the appearance of red-pink color of cellulose, hemicellulose and lignin in the area of cell walls and green-blue color in the vacant cell lumen. The aforementioned techniques focused on the effect of heat on wood covered with different preparation layers. Further studies may help to clarify why the same type of wood has different physical and mechanical properties when preserved under different conditions, especially high relative conditions, due to the changes in the chemical distribution of wood components in certain parts of the cell wall. There are many examples that prove that there is a diversity in wood properties and composition. For example, in a previous article the different parts of a coffin, which were made of several wood planks that varied in their physical properties due to different features of decay, the authors explained that the coffin seemed to have been made of various types of wood, but the microscopic investigation proved that all planks were made of sidder [44]. This confirms how the appearance of decayed wood can be very confusing at the first glance. In another article that mainly focused on FTIR analysis of different softwood samples, the FTIR results of Lebanese cedar wood varied to a wide extent, and it was very difficult to pinpoint in which parts of the cell wall the decay had occurred [22].

5. Conclusion

FTIR, FTIR-ATR and FTIR-ATR mapping are different analytical methods that were used to assess the chemical changes that occurred in both experimental wood samples and archaeological samples. FTIR analysis in this study provided a good indication of changes in wood cellulose, lignin and hemicellulose, in contrast to FTIR-ATR analysis which recorded only the surface changes of wood. ATR-FTIR mapping provided chemical images that show the changes of carbohydrate and lignin distribution in the wood cell walls. The calculated intensity ratios of carbohydrates to lignin in FTIR analysis were in agreeance with the ATR-FTIR chemical images. It is therefore recommended to use both methods together to understand the chemical changes in wood components when explaining the alterations in the different cell wall layers.

References

[1] Santon, K. (2007). *Tutankhamun: The treasures of the golden king*, Eng., Parragon Books, China.

[2] Reeves, N. (1990). *The complete Tutankhamun: The king, the tomb,the royal treasure*, Thames & Hudson, London.

[3] *http://www.griffith.ox.ac.uk/gri/gif-files/taa_i_2_11_94&95*.pdf. (14/9/2023).

[4] *http://www.griffith.ox.ac.uk/gri/gif-files/taa_i_2_11_88&89*.pdf. (14/9/2023).

[5] *http://www.griffith.ox.ac.uk/gri/tut-scans/TAA_i_3_ 9_1*.jpg. (14/9/2023).

[6] Rifai, M. & El Hadidi, N. (2010). Investigation and analysis of three gilded wood samples from the tomb of Tutankhamun. In: Dawson, J., Rozeik, C. & Wright, M. (eds.), *Decorated Surfaces on Ancient Egyptian Objects, Technology, Deterioration & Conservation*. Archetype Publications, pp. 16-24

[7] Abdallah, M. & Abdrabou, A. (2018). Tutankhamen's small shrines (naoses): Technology of woodworking and identification of wood species. *IJCS*. 9 (1): 91-104.

[8] Mohamed, H. (2018). *Study on the chemical effect of some consolidants on archaeological, softwood-applied on a selected object* (In Aribic), MA., Conservation dept., Faculty of Archaeology, Cairo Univ., Egypt.

[9] Gupta, S. & Saxena, V. (2011). Wood microstructure of ligneous species of Rhamnaceae from India. *J. of Tropical Forest Science*. 23 (3): 239-251.

[10] Saied, A., Gebauer, J., Hammer, K., et al. (2008). Ziziphus spina-christi (L.) willd: A multipurpose fruit tree. *Genetic Resources & Crop Evolution*. 55: 929-937.

[11] Abdulrahman, M., Zakariya, A., Hama, H., et al. (2022). Ethnopharmacology, biological evaluation, and chemical composition of *Ziziphus spina-christi* (L.) Desf.: A review. *Advances in Pharmacological & Pharmaceutical Sciences*, doi: 10.1155/2022/4495688.

[12] Pijut, P. (2000). *Cedrus*-the true cedars. *J. of Arboriculture*. 26 (4): 218-224.

[13] Lucas, A. (1948). *Ancient egyptian materials and industries* (3rd ed.), Edward Arnold LTD, London.

[14] Hafizoğlu, H. (1987). Studies on the chemistry of Cedrus libani A. Rich. *Wood Extractives of Cedrus libani*. 41 (1): 27-38.

[15] El Sherbiny, H. (2015). *Studies in dendro-Egyptology: The laboratory of tree-ring research Egyptian wooden collection*, M.Sc., GeoSciences dept., The University of Arizona, USA.

[16] El Hadidi, N. & Hamed, S. (2017). The effect of preparation layers on the anatomical structure and chemical composition of native Egyptian wood. In: Amenta, A. & Guichard, H. (eds.). *Proc. 1st Vatican Coffin Conf.*, Vol. I, Edizioni Musei Vaticani, Italy, pp. 199-210.

[17] Hamed, S. & El Hadidi, N. (2020). The use of Sem-Edx investigations in estimating the penetration depth of preparation layers within wood structure. *Advanced Research in Conservation Science*. 1: 1-15.

[18] Palache, C., Berman, H. & Frondel, C. (1951). *Dana's system of mineralogy*, Vol. 2, 7th ed., John Wiley & Sons, NY.

[19] Roscoe, H., Schorlemmer, C., Colman, H., et al. (1905). *A treatise on chemistry*. Vol. I: *The non-metallic elements*, 3rd ed., Macmillan, USA.

[20] Małachowska, E., Dubowik, M., Boruszewsk, P., et al (2021). Accelerated ageing of paper: Effect of lignin content and humidity on tensile properties. *Heritage Science.* 9 (132), doi: 10.1186/s40494-021-00611-3

[21] Matsuo, M., Yokoyama, M., Umemura, K., et al. (2011). Aging of wood-analysis of color changing during natural aging and heat treatment. *Holzforschung*. 65 (3): 361-368.

[22] El Hadidi, N. (2017). Decay of softwood in archaeological wooden artifacts. *Studies in Conservation*. 62 (2): 83-95.

[23] Papliaka, Z., Konstanta, A., Karapanagiotis, I., et al. (2017). FTIR imaging and HPLC reveal ancient painting and dyeing techniques of molluskan purple. *Archaeological & Anthropological Science*. 9: 197-208.

[24] Geffert, A., Geffertova, J. & Dudiak, M. (2019). Direct method of measuring the pH value of wood. *Forests*. 10 (10), doi.org/10.3390/f10100852

[25] Pandey, K. (1999). A study of chemical structure of soft and hardwood and wood polymers by FTIR spectroscopy. *J. of Applied Polymer Science*. 71(12): 1971-1975.

[26] Fackler, K., Stevanic, J., Ters, T., et al. (2010). Localisation and characterisation of incipient brown-rot decay within spruce wood cell walls using FT-IR imaging microscopy. *Enzyme and Microbial Technology*. 47 (6): 257-267.

[27] Chen, Z., Hu, T., Jang, H., et al. (2015). Modification of xylan in alkaline treated bleached hardwood kraft pulps as classified by attenuated total-internal-reflection (ATR) FTIR spectroscopy. *Carbohydrate Polymers.* 127: 418-426.

[28] Chen, S., Jiang, J., Liu, L., et al. (2010). 1,3-diamino-2-hydroxypropane-N,N,N′,N′-tetraacetic acid stabilized amorphous calcium carbonate: Nucleation, transformation and crystal growth. *Crystal Engineering Communications*. 12 (1): 234-241.

[29] Yao, C., Xie, A., Shen, Y., et al. (2013). Green synthesis of calcium carbonate with unusual morphologies in the presence of fruit extracts. *J. of the Chilean Chemical Society*. 58 (4): 2235-2238.

[30] Owen, N. & Thomas, D. (1989). Infrared studies of "hard" and "soft" woods. *Applied Spectroscopy*. 43 (3): 451-455.

[31] Alharbi, N. & Guirguis, O. (2019). Macrostructure and optical studies of hydroxypropyl cellulose in pure and nano-composites forms. *Results in Physics*. 15 (2), doi.org/10.1016/j.rinp.2019.102637

[32] Guirguis, O. & Moselhey, M. (2011). Optical study of poly(vinyl alcohol)/hydroxypropyl methylcellulose blends. *J. of Materials Science*. 46 (17): 5778-5779.

[33] Marchessault, R. (1962). Application of infrared spectroscopy to cellulose and wood polysaccharides. *Pure & Applied Chemistry*. 5 (1-2): 107-130.

[34] Kalutskaya, E. & Gusev, S. (1980). An infrared spectroscopic investigation of the hydration of cellulose. *Polymer Science USSR*. 22 (3): 550-556.

[35] Schwanninger, M., Rodrigues, J., Pereira, H., et al. (2004). Effects of short-time vibratory ball milling on the shape of FT-IR spectra of wood and cellulose. *Vibrational Spectroscopy*. 36 (1): 23-40.

[36] Popescu, M., Froidevaux, J., Navi, P., et al. (2013). Structural modifications of Tilia cordata wood during heat treatment investigated by FT-IR and 2D IR correlation spectroscopy. *J. of Molecular Structure*. 1033: 176-186.

[37] Huang, Y., Wang, L., Chao, Y., et al. (2012). Analysis of lignin aromatic structure in wood. *J. of Wood Chemistry & Technology.* 32 (4): 294-303.

[38] Liu, Y., Hu, T., Wu, Z., et al. (2014). Study on biodegradation process of lignin by FTIR and DSC. *Environmental Science & Pollution Research*. 21: 14004-14013.

[39] Zhao, J., Xiuwen, W., Hu, J., et al. (2014). Thermal degradation of softwood lignin and hardwood lignin by TGFTIR and Py-GC/MS. *Polymer Degradation & Stability*. 108: 133-138.

[40] Shi, J., Xing, D. & Li, J. (2012). FTIR studies of the changes in wood chemistry from wood forming tissue under inclined treatment. *Energy Procedia*. 16: 758-762.

[41] Reig, F., Adelantado, J. & Moreno, M. (2002). FTIR quantitative analysis of calcium carbonate (calcite) and silica (quartz) mixtures using the constant ratio method. Application to geological samples. *Talanta*. 58 (4): 811-821.

[42] Yang, H., Yan, R., Chen, H., et al. (2007). Characteristics of hemicellulose, cellulose and lignin pyrolysis. *Fuel*. 86 (12-13): 1781-1788.

[43] Unger, A., Schienwiend, A. & Unger, W. (2001). *Conservation of wood artifacts: A handbook*, Springer Science & Business Media, Germany.

[44] El Hadidi, N., Darwish, S., Ragab, M., et al. (2019). Beyond the visible, merging scientific analysis and traditional methods for the documentation of the anthropoid coffin of Amenemhât. In: Strudwick, H. & Dawson, J. (eds.); *Ancient Egyptian Coffins Past - Present - Future*, Oxbow Books, Oxford, pp. 13-21.